Free Radical Biology and Medicine 227 (2025) 42–51

Contents lists available at ScienceDirect

Free Radical Biology and Medicine

journal homepage: www.elsevier.com/locate/freeradbiomed

Protective effects of olive oil antioxidant phenols on mercury-induced phosphatidylserine externalization in erythrocyte membrane: Insights into scramblase and flippase activity

Pasquale Perrone [a,1], Rosaria Notariale [b,1], Gennaro Lettieri [c], Luigi Mele [d], Valeria La Pietra [e], Marina Piscopo [c], Caterina Manna [a,*]

[a] Department of Precision Medicine, School of Medicine, University of Campania "Luigi Vanvitelli", 80138, Naples, Italy
[b] Department of Biology and Evolution of Marine Organisms, Stazione Zoologica Anton Dohrn, Villa Comunale, 80121, Naples, Italy
[c] Department of Biology, University of Naples Federico II, 80126, Naples, Italy
[d] Department of Experimental Medicine, University of Campania "Luigi Vanvitelli", Italy
[e] Department of Pharmacy, University of Naples Federico II, via D. Montesano 49, 80131, Napoli, NA, Italy

ARTICLE INFO

Keywords:
Antioxidant
ATP11C
Glutathione
Hydroxytyrosol
Mercury chloride
Molecular docking
Olive oil phenols
Oxidative stress
Phosphatidylserine
PLSCR1

ABSTRACT

In several physiopathological processes, phosphatidylserine (PS), normally sequestered to the inner leaflet of the plasma membrane, becomes exposed to the cell surface. In erythrocytes (RBC), PS externalization is a crucial event for the removal of aged/damaged cells but can also be associated with increased prothrombotic activity. Structurally related olive oil antioxidants, including hydroxytyrosol (HT), are able to significantly reduce the percentage of PS-exposing RBC, when cells are exposed to toxic compounds such as the heavy metal mercury (Hg). The aim of the present study was to identify the molecular mechanisms underlying the protective effect, with a focus on two different phospholipid translocases, the ATP-dependent flippase ATP11C and the calcium-dependent scramblase PLSCR1, which are responsible for PS internalization and exposure, respectively. In addition to HT, its monophenol analogue, tyrosol, and its *in vivo* metabolite, homovanillic alcohol, were also tested. Our investigation revealed that exposure of human intact RBC to $HgCl_2$ induced a decrease in flippase activity and an increase in scramblase activity, and that all the selected phenols restored the control activity, regardless of their different scavenging properties. Interestingly, all phenols restored the ATP level of control cells, which were significantly reduced by $HgCl_2$ treatment. Conversely, no variation in intracellular calcium was observed under our experimental conditions. Additionally, all phenols restored the glutathione levels, significantly reduced in the presence of $HgCl_2$. In line with the data on the enzymatic activity, Western blotting analysis indicated changes in the membrane expression of the two enzymes, alterations prevented by antioxidant pre-treatment. Finally, molecular docking analysis suggests that the tested antioxidants may be able to directly interact with ATP11C. Our findings provide an experimental basis for the use of olive oil bioactive compounds in nutritional/nutraceutical strategies for the prevention of Hg-related toxicity, particularly in relation to the cardiovascular tissues.

ABBREVIATIONS

ATP11C	VI type 11C ATPase
CVD	Cardiovascular disease
GSH	Glutathione
HA	Homovanillic alcohol

(*continued on next column*)

(*continued*)

Hg	Mercury
HT	Hydroxytyrosol
MV	Microvescicles
NBD-PC	Nitrobenzoxadiazole-labelled PC
NBD-PS	Nitrobenzoxadiazole-labelled PS

(*continued on next page*)

* Corresponding author.
E-mail addresses: pasqualeperrone1995@gmail.com (P. Perrone), notarialer@gmail.com (R. Notariale), gennarole@outlook.com (G. Lettieri), luigi.mele86@gmail.com (L. Mele), valeria.lapietra@unina.it (V. La Pietra), marina.piscopo@unina.it (M. Piscopo), caterina.manna@unicampania.it (C. Manna).
[1] These authors contributed equally to this work.

https://doi.org/10.1016/j.freeradbiomed.2024.11.047
Received 2 May 2024; Received in revised form 21 November 2024; Accepted 26 November 2024
Available online 27 November 2024

(*continued*)

PC	Phosphatidylcholine
PLSCR1	Phospholipid scramblase
PS	Phosphatidylserine
RBC	Erythrocytes
TYR	Tyrosol

1. Introduction

Phosphatidylserine (PS) is a crucial component of the plasma membrane that plays a key role in red blood cells (RBC) physiopathology [1]. The two layers of the cell membrane, the outer and the inner, differ not only in their protein content but also in their lipid composition. This marked asymmetry reflects the distinct functions of the two layers, with the majority of PS typically located on the cytoplasmic side of the cell membrane under normal physiological conditions [2]. The loss of membrane asymmetry in ageing cells has significant physiological implications, leading to increased exposure of PS on the cell surface. This exposure of PS serves as a critical mechanism regulating the half-life of RBC. Indeed, phagocytosis of RBC by macrophages is triggered by PS exposure, which acts as an 'eat me' signal [3,4]. In addition, PS-related alteration in membrane asymmetry, may play a pivotal role in cardiovascular disease (CVD) [5]. Elevated PS exposure, is considered a critical event in enhancing of prothrombotic activity of RBC, affecting hemostasis and coagulation processes [6]. Under physiological conditions, RBC interact minimally with endothelial cells. However, increased PS exposure promotes RBC adhesion to endothelial cells, contributing to thrombus formation and subsequent microvascular occlusion [7]. Moreover, the presence of PS on the outer surface of the RBC membrane provides a binding site for the assembly of the prothrombinase complex, which in turn triggers the generation of thrombin, thereby stimulating the coagulation cascade [8].

The movement of lipids across the plasma membrane is primarily regulated by two types of enzymes: flippase and scramblase [9]. Scramblase facilitate the random diffusion of phospholipids, including PS and phosphatidylcholine (PC), in both directions across the plasma membrane. Notably, the Ca^{2+}-dependent phospholipid scramblase (PLSCR1) family plays a key role in this process [10].

The distribution of PS in the inner leaflet of the membrane, achieved by displacing it from the outer leaflet of the cell membrane, is mediated by flippase, which belong to the type IV P family of ATPases (P4-ATPases) [11]. In human RBC, the major enzyme responsible for the PS 'flipping' process is the class VI type 11C ATPase (ATP11C) [12].

Various substances, including heavy metals like mercury (Hg), can trigger an increase in PS exposure [13]. Hg, an environmental pollutant found in the atmosphere, soil and water, poses serious threats to both ecosystems and human health, causing harmful short- and long-term effects [14]. Recently, significant attention has been paid towards on the direct effect of Hg on cardiovascular tissues, including endothelial cells, which increases the risk of CVD [15]. The molecular mechanisms underlying Hg-induced cytotoxicity are complex; however, it is known that Hg can rapidly react to the sulfhydryl group (SH) present in various molecules, including proteins and low molecular weight molecules such as glutathione (GSH), thereby interfering with key metabolic processes and the antioxidant defense system [16]. Interestingly, Hg has also been found to alter the activity of both flippase and scramblase, leading to increased PS exposure on the outer surface of the cell membrane [17].

In recent years, there has been a growing interest in exploring the potential of natural compounds to reduce heavy metal toxicity. In this regard, our group has demonstrated that structurally related phenolic antioxidants present in olive oil can reduce PS exposure in $HgCl_2$-treated RBC. Specifically, hydroxytyrosol (HT), exhibits significant protective properties against $HgCl_2$-induced damage in RBC, including oxidative stress, metabolism and morphology [13,18].

Based on these findings, the present study aimed to identify the molecular mechanism underlying the protective effect of antioxidant olive oil phenols on PS exposure in human RBC treated with $HgCl_2$. Also, we compared the protective effect of cell pre-treatment with HT and its natural monophenol analogue tyrosol (TYR) and its *in vivo* metabolite homovanillic alcohol (HA), endowed with different scavenging capacities, on the enzyme activity and expression levels of ATP11C and PLSCR1. Furthermore, since ATP11C is an ATP-dependent enzyme and PLSCR1 is a Ca^{2+}-dependent enzyme, intracellular ATP and Ca^{2+} levels were also assessed in $HgCl_2$-treated and HT, TYR and HA-pre-treated RBC. In order to assess whether the antioxidant function of the phenols plays a key role in the molecular mechanism under our conditions, intracellular GSH levels were assessed. Finally, molecular docking studies were conducted to identify the possible binding interactions between these compounds and the flippase target.

2. Materials and methods

2.1. Chemicals and solutions

Phosphate-buffered saline (PBS), bovine serum albumin (BSA), DTNB (5,5-dithiobis (2-nitrobenzoic acid), $HgCl_2$, HT, TYR and HA were from Sigma Chemical Co. Nitrobenzoxadiazole-labelled PS (NBD-PS) and Nitrobenzoxadiazole-labelled PC (NBD-PC) were from Avanti Polar Lipids. Bradford reagent and Tris-Glycine gradient gels were from Thermo Fisher Scientific (Waltham, MA, USA). Coomassie Brilliant Blue R250 was from Fluka Chemie (Buchs, Switzerland). Tween-20 was bought from Roche- Diagnostic (Mannheim, Germany). Rabbit anti-ATP11C antibody was from ThermoFisher. Rabbit anti-PLSCR1 antibody, rabbit anti-GAPDH antibody, mouse anti-rabbit HRP polyclonal immunoglobulin and goat anti-rabbit HRP polyclonal immunoglobulin were from ElabScience. Fluo-3/AM was from Immunotools (Friesoythe, Germany). ATP Assay kit was from Cayman Chemical.

$HgCl_2$ was prepared in distilled water and diluted from 100 mM stock Solution. HT, TYR and HA were prepared in dimethyl sulfoxide (DMSO) and diluted from 100 mM stock Solution.

2.2. Preparation of RBC and treatment with $HgCl_2$

Whole blood was obtained with informed consent from healthy volunteers at the University of Campania 'Luigi Vanvitelli' (Naples, Italy). It was collected in tubes with heparin and centrifuged at 2000×*g* for 10 min at 4 °C. After removal of the buffy coat, the RBC fraction was washed three times with isotonic saline solution (0.9 % NaCl) and resuspended in Krebs solution containing (mM) NaCl 125, KCl 4, $MgSO_4$ 1, Hepes 32, $CaCl_2$ 1, glucose 5; pH 7.4 to obtain a different hematocrit as required (0.4-2-10 %). RBC were incubated for 1 h at 37 °C with $HgCl_2$ (5 μM) and different concentrations of the selected phenolic compounds HT, HA and TYR (5–10 μM). Incubation of control RBC only with phenols does not modify any of the markers utilized [Supplementary materials (SM)].

2.3. Measurement of flippase and scramblase activities

We measured phospholipid translocation according to the method described by *Seki* et al. [19]. After the respective treatments, RBC washed at 2 % hematocrit were preincubated in 0.5 mL PBSG (PBS containing 20 mM glucose) at 37 °C. Subsequently, 0.5 μL of NBD-PS for the flippase activity assay or NBD-PC for the scramblase activity assay were added and incubated at 37 °C for 20 min. Aliquots of the cell suspension (20 μL) were then mixed with PBS in the presence or absence of 1 % BSA to remove residual NBD-PS/PC in the outer leaflet. In this way it is possible to show that the remaining fluorescence associated with the cells represents the PS/PC that has translocated to the inner leaflet [12].

The amount of internalized probe was calculated by dividing the

fluorescence intensity associated with the RBC before and after back-extraction with BSA. Samples were analyzed on the FACScalibur flow cytometer and evaluated using FlowJo V10 software. For all samples, 100,000 cells were analyzed.

2.4. Intracellular ATP levels measurement

The intracellular ATP level was measured with the ATP Assay kit using the manufacturer's instructions. Briefly, after the respective incubation conditions, RBC (0.4 % hematocrit) were washed with cold PBS and lysed with cold ATP 1X Sample buffer. 1 μL of each sample and standards were placed in a 96-well plate added to 100 μL of freshly prepared reaction mixture (1X ATP Detection Assay Buffer, D-Luciferin and Luciferase) and the plate was incubated at room temperature (RT) for 20 min, protected from light. The intensity of luminescence was detected by the Spark 10 M multimodal microplate reader (TECAN) and the ATP concentration was calculated according to the manufacturer's instructions.

2.5. Intracellular Ca^{2+} measurement

Measurement of intracellular calcium levels was obtained using the Fluo-3 probe as reported in *Officioso* et al. [20]. After incubation under the respective conditions, 100 μl of RBC suspension (2 % hematocrit) was washed in Krebs solution and then loaded with Fluo-3/AM in Krebs solution containing 5 μM Fluo-3/AM. Subsequently, the cells were incubated at 37 °C for 30 min and washed in Krebs solution containing 5 mM $CaCl_2$. RBC loaded with Fluo-3/AM were resuspended in 200 μl Krebs solution. Fluorescence intensity was measured with an excitation wavelength of 488 nm and an emission wavelength of 530 nm on a FACS Calibur.

2.6. Preparation of RBC membranes and protein extraction

Membrane protein extraction was performed according to *Notariale* et al. [21] After treatment with $HgCl_2$, RBC (10 % hematocrit) were washed twice with isotonic saline solution (0.9 % NaCl) and centrifuged at 2000 g for 10 min at 4 °C. The samples are incubated for 1 h at 4 °C with a hypotonic 0.1x PBS solution under agitation to achieve cell lysis. Membranes were separated from intracellular contents by ultracentrifugation at 21,500 g, 75 min, 4 °C. We separated the supernatant, which contains the cytosolic fraction, from the lower part containing the membranes. Subsequently, the membranes were washed eight times by centrifugation at 21,500 g, 30 min, 4 °C to remove as much hemoglobin as possible from the membranes. Total membrane proteins were then extracted from the pelleted membranes under native conditions using DC buffer: 1 % DC in 50 mM Tris-HCl, 150 mM NaCl, pH 8.1. A final centrifugation was performed at 21,500 g, 30 min, 4 °C. Protein concentrations were measured by absorbance with the Bradford reagent and the ThermoFisher Elios spectrophotometer.

2.7. SDS-page analysis

Total membrane protein extracts were analyzed by SDS-PAGE. 40 μg of protein from each sample and 10 μL of 1X Laemmli buffer were boiled at 100 °C for 10 min and then loaded onto 1.0 mm 4–8% Tris-Glycine gradient gels. The electrophoretic run was performed in Tris Glycine 2X run buffer at 150 V for approximately 2 h.

After separation, the proteins were stained with Coomassie Brilliant Blue R250 and acquired with a GelDoc system using the ImageLab 6.0.1 software programme (BioRad, Hercules, CA, USA).

2.8. Western Blotting

Western Blotting analyses were performed on nitrocellulose membranes (1 h transfer at 10 V in Tris-glycine buffer in a Mini Trans-Blot electrophoretic transfer cell). The membranes were rinsed three times for 10 min in TBS-T (1x TBS, 0.1 % Tween-20) and blocked with 5 % skim milk in TBS-T for 1 h at RT under agitation. They were then incubated separately with the following primary monoclonal antibodies in TBS-T: rabbit anti-ATP11C antibody (1:500), rabbit anti-PLSCR1 antibody (1:1000) and rabbit anti-GAPDH antibody (1:4000). After one night, the membranes were again rinsed three times for 10 min in TBS-T. The membranes were then incubated with secondary antibodies (mouse anti-rabbit HRP polyclonal immunoglobulin) (goat anti-rabbit HRP polyclonal immunoglobulin) diluted to January 2000 and 1/4000 respectively in 3 % skimmed-milk buffer in TBS-T for 2 h at RT with agitation. Finally, the membranes were washed three times in TBS-T at RT. The HRP reaction was detected using a chemiluminescence kit (ECL Western Blotting Substrate, Pierce, Waltham, MA, USA) and images were acquired using the ChemiDoc system (Bio-Rad, Hercules, CA, USA). The immunopositive signal corresponding to the enzymes was quantified by densitometric analysis using Image Lab 6.0.1 software. The levels of ATP11C and PLSCR1 were compared with the intensity of GAPDH.

2.9. Reduced glutathione assay

The intracellular GSH content was assessed according to *Tortora* et al. [22]. After incubation under the respective conditions (10 % hematocrit), the samples (0.25 mL) were centrifuged for 5 min at 800×*g* and then the supernatant was removed. The RBC were lysed with 0.6 mL of cold water and the proteins were precipitated by the addition of 0.6 mL of a cold solution of metaphosphoric acid (1.67 g metaphosphoric acid, 0.2 g EDTA and 30 g NaCl in 100 mL water). The samples were placed at 4 °C for 10 min, and a subsequent centrifugation at 18,000×*g* for 10 min removed the precipitated proteins. Finally, 0.45 mL of supernatant was mixed with an equal volume of 0.3 M Na_2HPO_4. To determine the reduced GSH, 0.1 mL of a DNTB solution (20 mg DTNB plus 1 % sodium citrate in 100 mL water) was added to the solution. After 10 min of incubation at RT, the absorbance of the samples was measured at a wavelength of 412 nm.

2.10. Molecular modeling

We employed a multi-step approach to perform a blind docking of HT against the flippase protein using SiteMap and Glide 5.5 program within the Schrödinger package. Maestro v. 12.7.156 (Maestro, Schrödinger, LLC, New York, NY, 2021) was employed as the graphical user interface, and Fig. 8 representing the most probable binding mode of HT was rendered by the Chimera software package [23]. Docking calculations were also performed for HA and TYR.

Ligand and Protein Setup. As for the HT, HA and TYR structure: the molecules were built and prepared through the LigPrep (LigPrep, Schrödinger, LLC, New York, NY, 2021) module of Maestro, employing the OPLS2005 force field. Epik (Epik, Schrödinger, LLC, New York, NY, 2021) is used to evaluate the ligands' pKa at neutral pH and so to properly describe their protonation state. Then, the obtained ligands are optimized at molecular mechanics level through the MacroModel (MacroModel, Schrödinger, LLC, New York, NY, 2021) program included in the Schrödinger suite of programs.

The target protein (PDB code: 7BSU) [24] was prepared using the protein preparation wizard in Maestro 9.0.211. Water molecules were removed, hydrogen atoms were added, and minimization was performed until the rmsd of all heavy atoms was within 0.3 Å of the crystallographic positions.

Ligand Pocket finding and docking setup. A SiteMap (Schrödinger Release 2024–1: SiteMap, Schrödinger, LLC, New York, NY, 2024) run was conducted using the Schrödinger software suite to identify potential binding pockets within the protein structure. This analysis identified five distinct binding sites. Subsequently, grid maps were generated for each identified binding pocket to define the spatial and energetic

properties of the binding sites. The grid maps were then utilized as input for the Glide docking software, which employs a flexible docking algorithm to predict the binding modes and affinities of small molecules within the defined binding pockets. Notably, each grid map was processed concurrently, enabling high-throughput virtual screening across multiple binding sites simultaneously thanks to the virtual screening workflow.

At the end, a specific docking calculation only into the pocket nearby the metal ion Mg^{2+} was performed. All molecular docking calculations were performed with the aid of Glide 5.5 in SP mode [25,26], using Glidescore for ligand ranking, letting all the other parameters as default. The receptor was kept fixed, the ligand was treated as flexible, and no other constraints were added.

2.11. Statistical analyses

Data evaluations were expressed as means ± S.D. of 3 independent experiments performed in triplicate with RBC from different donors. The significance of differences was determined by one-way ANOVA followed by a post Tukey's multiple comparisons test. GraphPad Prism 10 was utilized for statistical analysis.

3. Results

3.1. Measurement of flippase and scramblase activity

In order to unveil any possible protective effects of the selected phenolic compounds on RBC upon heavy metal treatment, we firstly measured any changes in flippase activity following treatment of the RBC with 5 μM of $HgCl_2$ with or without phenolic compounds. The "flip-flop" activity of the enzyme was measured by flow cytometry, monitoring the internalization of NBD-PS. The fluorescent probe was loaded onto the membranes of control RBC, $HgCl_2$-treated RBC and cells pre-treated with HT, TYR and HA. In control samples (Fig. 1), the percentage of NBD-PS present in the inner leaflet exceeds 90 %, indicating normal flippase activity. In contrast, in samples treated with $HgCl_2$, the amount of NBD-PS present in the inner leaflet is significantly lower, indicating a decrease in the enzyme activity. Interestingly, samples pre-treated with the three phenolic compounds show an almost complete recovery of the enzyme activity, and this effect is concentration dependent. In particular, HT and HA show similar effect, with almost complete recovery at a concentration of 10 μM, but with a protective effect already observed at 5 μM. TYR also appears protective against $HgCl_2$-induced alteration of flippase activity, although to a lesser extent, with a significant value at 10 μM.

As previously reported, PS transport is mediated by both flippase and scramblase. Therefore, scramblase activity has also been assessed. To discriminate the activity of these two enzymes, the fluorescent analogue of PC, namely NBD-PC, was used, as this phospholipid is solely transported by scramblase. Changes in enzyme activity were then determined in samples treated with $HgCl_2$ and pre-treated with HT, TYR and HA. In Fig. 2 as expected, since this enzyme translocate PC randomly, the control samples showed that the percentage of NBD-PC found in the inner leaflet is approximately 50 %, indicating normal scramblase activity. Conversely, in samples treated with $HgCl_2$, the amount of NBD-PC present in the inner leaflet is significantly higher, indicating a significant alteration in the activity of this enzyme. Again, all three selected phenolic compounds demonstrate a concentration-dependent protective effect.

3.2. Measurement of intracellular ATP and calcium levels

As aforementioned, ATP11C is an ATP-dependent enzyme while PLSCR1 is a Ca^{2+}-dependent enzyme, thus, intracellular ATP and Ca^{2+} levels were assessed, to determine the possible mechanisms of action for effects described above. Precisely, possible changes in intracellular ATP levels under our conditions were investigated. As depicted in Fig. 3, treatment with $HgCl_2$ induced a slight depletion of ATP levels even after only 1 h of treatment. Furthermore, it is noteworthy to note that the presence of the selected phenols led to a total restoration of ATP levels even at low concentrations (5 μM).

$HgCl_2$ treatment is known to induce an increase in intracellular calcium concentrations in RBC [17]. However, as shown in Fig. 4, no significant increase in intracellular calcium was observed under the same experimental conditions with 5 μM of $HgCl_2$. The figure also

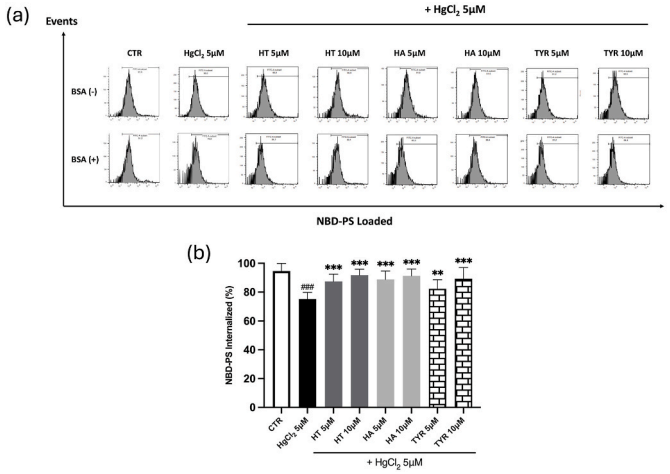

Fig. 1. Effect of HT and its analogues on $HgCl_2$-induced alteration in flippase activity. Cells were treated with $HgCl_2$ in the presence of increasing concentrations of HT, TYR and HA and flippase activity was analyzed using NBD-PS. (a) Original histograms of NBD-PS primary fluorescence data derived from flow cytometry. Data from samples processed in the absence (top) and presence (bottom) of BSA. (b) Histogram of the effect of phenols on $HgCl_2$ treatment. Data are expressed as mean ± SD (n = 9). Statistical analysis was performed with one-way ANOVA followed by Tukey's test. ### ($p < 0.001$) indicates a significant difference from CTR. *** ($p < 0.001$) and ** ($p < 0.01$) indicates a significant difference from $HgCl_2$ treatment.

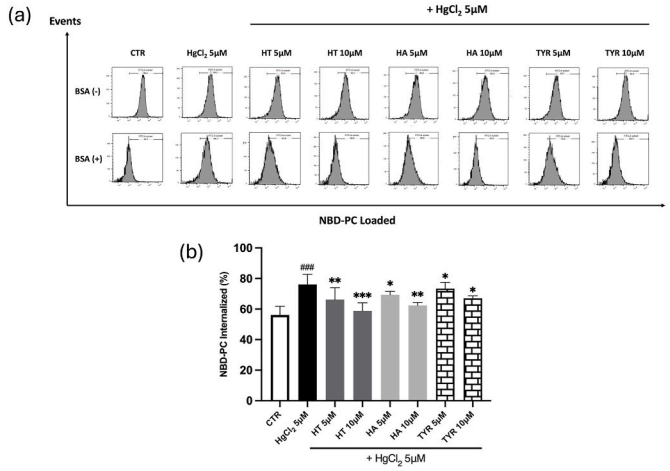

Fig. 2. Effect of HT and its analogues on $HgCl_2$-induced alteration in scramblase activity. Cells were treated with $HgCl_2$ in the presence of increasing concentrations of HT, TYR and HA and scramblase activity was analyzed using NBD-PC. (a) Original histograms of NBD-PC primary fluorescence data derived from flow cytometry. Data from samples processed in the absence (top) and presence (bottom) of BSA. (b) Histogram of the effect of phenols on $HgCl_2$ treatment. Data are expressed as mean ± SD (n = 9). Statistical analysis was performed with one-way ANOVA followed by Tukey's test. ### ($p < 0.001$) indicates a significant difference from CTR. *** ($p < 0.001$), ** ($p < 0.01$) and * ($p < 0.05$) indicates a significant difference from $HgCl_2$ treatment.

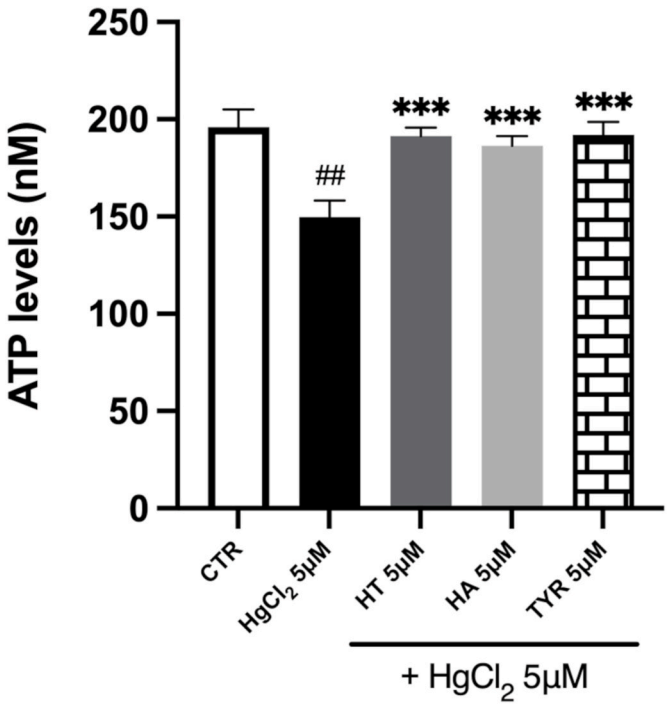

Fig. 3. Effect of HT and its analogues on $HgCl_2$-induced ATP decrease in RBC. Cells were treated with $HgCl_2$ in the presence of HT, TYR and HA. Data are the means ± SD (n = 9). Statistical analysis was performed with one-way ANOVA followed by Tukey's test. ## ($p < 0.01$) indicates a significant difference from CTR. *** ($p < 0.001$) indicates a significant difference from $HgCl_2$ treatment.

demonstrates the effect of the ionophore A23187 on intracellular calcium concentration, which was used as a positive control.

3.3. Western Blotting analysis

As we aimed to discern the mechanism of action underlying the observed effects, the significant alterations in enzyme activity prompted further investigation. Hence, we employed Western blotting to examine the expression levels of ATP11C and PLSCR1 on the RBC membrane under different conditions.

As shown in Fig. 5, treatment of the samples with $HgCl_2$ induces a significant reduction in the expression level of ATP11C. On the other hand, pre-treatment with HT, TYR and HA resulted in an almost complete restoration of the control condition. Interestingly, a concentration-dependent behavior is evident. Across all three cases, the use of a concentration of 10 μM shows a more pronounced effect, although pre-treatment with a phenol concentration of 5 μM also demonstrates a significant effect on the ATP11C expression level.

In addition, as illustrated in Fig. 6, treatment with $HgCl_2$ significantly increases the expression level of PLSCR1. Conversely, pre-treatment with HT at 10 μM restores levels akin to observed in untreated samples. Furthermore, comparable effects were observed with pre-treatment using HA and TYR at 10 μM. In both cases, a statistically significant protective effect on PLSCR1 expression level was observed compared to $HgCl_2$ treatment, with HT and HA exhibiting a slightly superior effect over TYR. Interestingly, no effect was observed with pre-treatment using the three selected phenolic compounds at 5 μM.

3.4. Reduced glutathione measurement

Considering the pivotal role GSH depletion in $HgCl_2$-induced toxicity, resulting in the impairment of the antioxidant defense system,

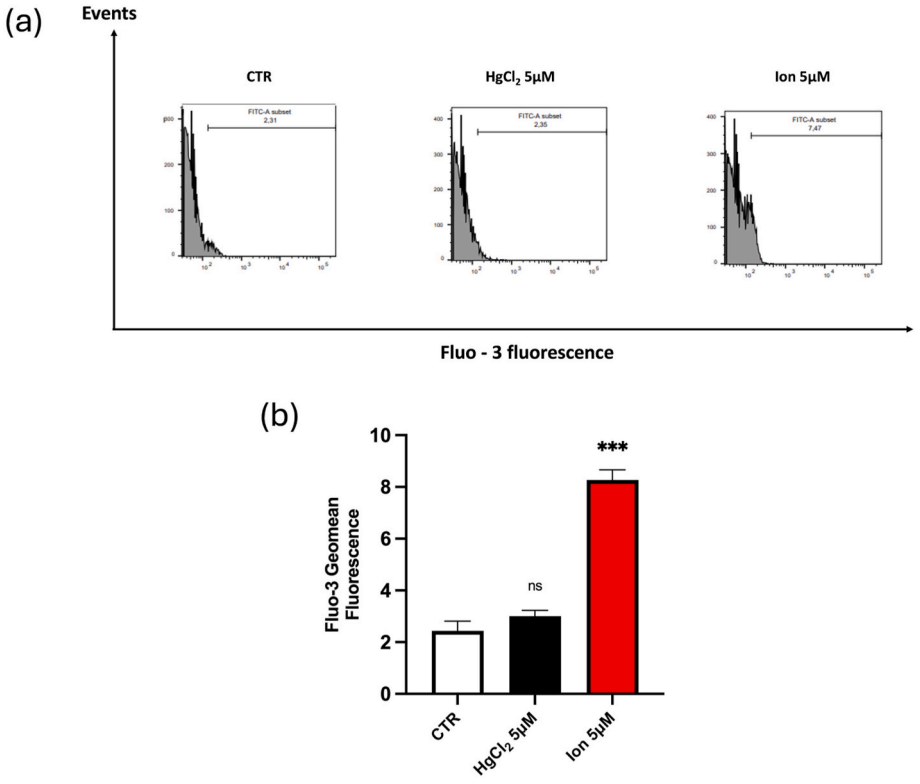

Fig. 4. Effect of $HgCl_2$ on intracellular Ca^{2+} levels. Cells were treated with $HgCl_2$ and Ionophore A23187 and intracellular Ca^{2+} levels were analyzed using the fluorescent probe Fluo-3 AM. (a) Original histograms of Fluo-3 AM primary fluorescence data derived from flow cytometry. (b) Histogram of the effect of $HgCl_2$ treatment. Data are expressed as mean ± SD (n = 9). Statistical analysis was performed with one-way ANOVA followed by Tukey's test. *** ($p < 0.001$) indicates a significant difference from CTR and ns ($p > 0.05$) indicates no significant difference from CTR.

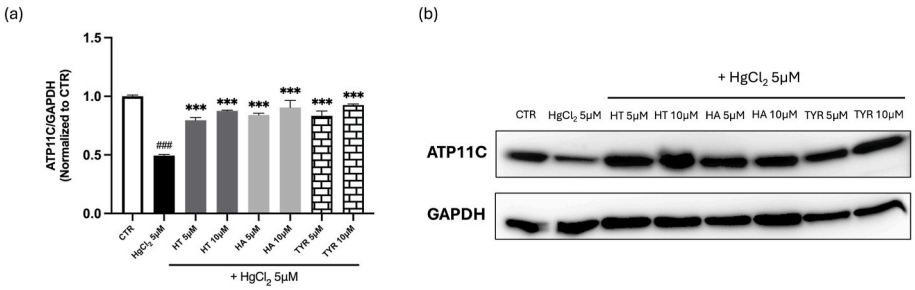

Fig. 5. Western blot analysis of ATP11C from human RBC. Cells were treated with $HgCl_2$ in the presence of increasing concentrations of HT, TYR and HA. (a) Densitometric analysis expressed as mean ± SD (n = 9). (b) Representative analysis of an experiment of nine replicates. Statistical analysis was performed with one-way ANOVA followed by Tukey's test. ### ($p < 0.001$) indicates a significant difference from CTR. *** ($p < 0.001$) indicates a significant difference from $HgCl_2$ treatment.

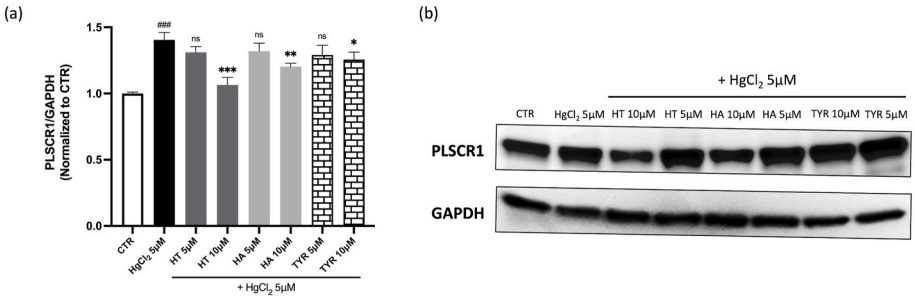

Fig. 6. Western blot analysis of PLSCR1 from human RBC. Cells were treated with $HgCl_2$ in the presence of increasing concentrations of HT, TYR and HA. (a) Densitometric analysis expressed as mean ± SD (n = 9). (b) Representative analysis of an experiment of nine replicates. Statistical analysis was performed with one-way ANOVA followed by Tukey's test. ### ($p < 0.001$) indicates a significant difference from CTR. *** ($p < 0.001$), ** ($p < 0.01$) and * ($p < 0.05$) indicates a significant difference from $HgCl_2$ treatment. Ns ($p > 0.05$) indicates no significant difference from $HgCl_2$ treatment.

we investigated the potential protective effects of HT and its analogues against this specific $HgCl_2$-induced metabolic alteration. As shown in Fig. 7, following 1 h of exposure of RBC to the heavy metal, a severe depletion of GSH was observed. Interestingly, all the selected phenols were able to partially restore the cellular GSH content, with a dose-dependent trend.

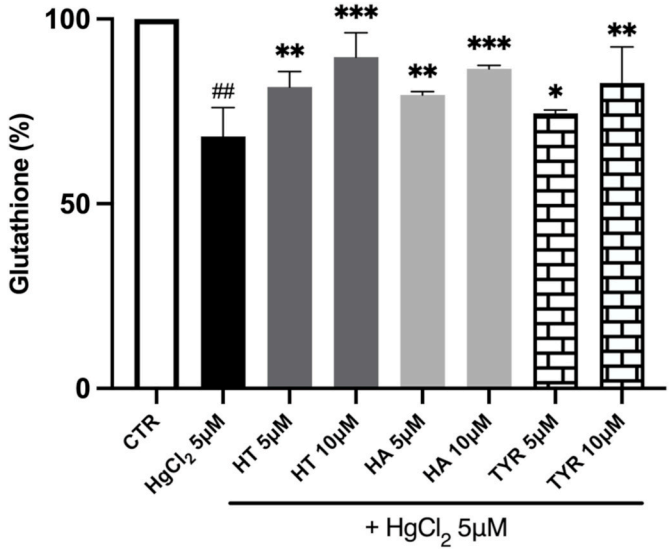

Fig. 7. Effect of HT and its analogues on $HgCl_2$-induced GSH decrease in RBC. Cells were treated with $HgCl_2$ in the presence of HT, TYR and HA. Data are the means ± SD (n = 9). Statistical analysis was performed with one-way ANOVA followed by Tukey's test. ## ($p < 0.01$) indicates a significant difference from CTR. *** ($p < 0.001$), ** ($p < 0.01$) and * ($p < 0.05$) indicates a significant difference from $HgCl_2$ treatment.

3.5. Molecular modeling

Considering the biological activity observed with HT, we hypothesized a potential direct interaction between this phenol compound and the flippase protein. To elucidate the binding mechanism of HT to the flippase protein at the atomic level, molecular docking studies were conducted utilizing the ATP11C X-ray structure (PDB code: 7BSU). Additionally, we speculated that a plausible allosteric interaction could underlie the observed restoration of protein activity.

Firstly, we conducted a SiteMap analysis using the Schrödinger package to delineate potential binding sites within the proteins. This analysis revealed the presence, besides the main catalytic pocket, of other five putative binding pockets (Fig. 8A). Then, grids were generated at these identified sites, and HT was docked into each using the Virtual Screening Workflow, that allows to perform an ensemble docking to multiple grids in a single job. Notably, this automated procedure resulted in HT preferentially localizing in the pocket nearby the Mg^{2+} ion. Further docking simulations were performed using Glide software solely within this pocket, yielding multiple HT poses that were structurally superimposable. These poses revealed HT's proximity not only to the metal ion but also to the side chains of T250, T174, A176, S177, E837, and K252 residues (Fig. 8B). Particularly, H-bonds are found between the catecholic oxygens and the K252 protonated group and T174 and between the HT hydroxyl group and the E837. Interestingly, similar results were obtained with the docking of HA and TYR, whose binding position is closely aligned with that of HT (data not shown).

Additionally, we conducted a comprehensive analysis of cysteine residues within ATP11C. A total of 23 cysteines were identified, 6 of which are bound together by disulfide bridges. Using Chimera software, all cysteines were visualized, revealing that most are inward-oriented, with two key exceptions: C914, located near but outside the catalytic

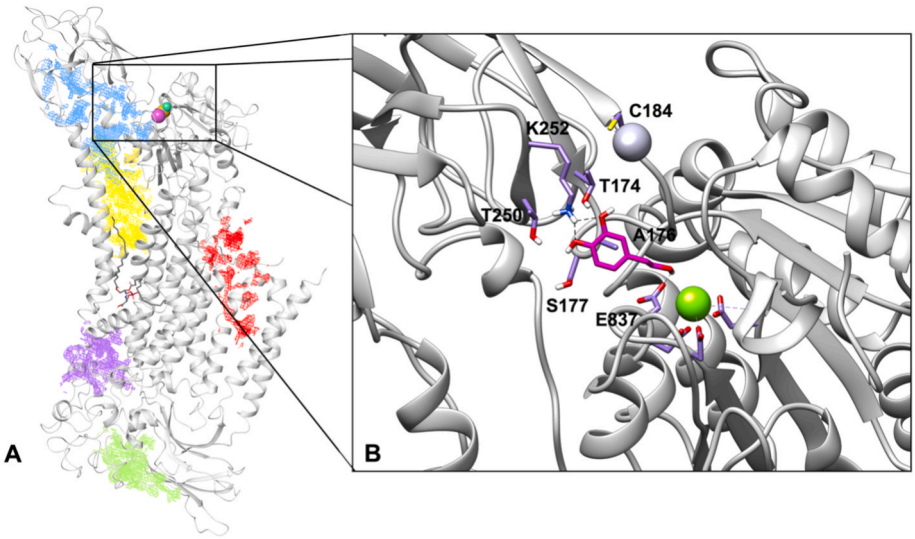

Fig. 8. A) Representation of the five putative binding pockets, which are shown as light blue, yellow, red, violet and green meshes, respectively. The co-crystalized ligand is also present to indicate the location of the main binding site. b) Best binding pose of HT into the pocket nearby the Mg^{2+} ion. ATP11C is represented as gray cartoon, HT in magenta sticks, while the protein interacting residues in slate sticks. H-bonds are shown as black dashed lines.

pocket, and C184, situated in the pocket near the Mg^{2+} ion in a really solvent-accessible area (see Fig. 16 in SM). Interestingly, C184 is in proximity of the site where HT preferentially binds (distance (C184-S, T174-Cγ) = 4.26 Å; distance (C184-S, K252-Cb) = 4.28 Å). This suggests that Cys184 may be a critical site for the interaction between Hg^{2+} and ATP11C, potentially affecting Mg^{2+} binding. A detailed image of the cysteine mapping is provided in the SM, and in Fig. 8B, HT can be observed bound in the pocket, near the Mg^{2+} ion and a hypothetical Hg^{2+} ion bound to Cys184.

4. Discussion

Recent studies highlight the effectiveness of natural products, including olive oil phenolic compounds, in combatting diseases like heavy metal poisoning [27]. HT, found in olive oil, exhibits anti-inflammatory, anti-proliferative, and antimicrobial properties [28–30]. It shows promise in protecting against various cancers and neurodegenerative diseases like Parkinson's [31–36]. HT plays a vital role in cardiovascular health by reducing risk factors such as high LDL cholesterol levels [37]. More recent findings also indicate that HT induces a reduction in NF-κB activation by downregulating mRNA levels of cytokines, chemokines and adhesion molecules [38]. Clinical studies support its efficacy in lowering LDL cholesterol, Apo B, and plasma Reactive C Protein levels [39].

More recently data from our group have shown that structurally related antioxidant are able to counteract the increased PS exposure induced in human RBC by different stressors, such as $HgCl_2$ and elevated Ca^{2+} concentration [13]. However, the mechanisms underlying this protective effect are not fully understood. In this paper we report new insights on the potential molecular mechanisms that could explain the observed effect focusing on the activities of phospholipid translocases.

Our data show that treatment with $HgCl_2$ induced a decrease in PS transport on the inner leaflet of the RBC plasma membrane, while PC levels found on the outer leaflet were significantly higher. It is clear, therefore, that $HgCl_2$ induces an alteration in both enzymatic activities, according to *Lim* et al. [17] reporting that flippase activity was inhibited by $HgCl_2$, while scramblase was activated in a concentration-dependent manner. Interestingly, a similar effect was found when RBC were treated with a different heavy metal such as lead [40]. It should be emphasized that living systems interact in the environment not only with a single heavy metal, but more often with a cocktail of compounds that can have synergistic adverse effects on the organism [41].

Here we report that pre-treatment with olive oil phenolic compounds restored the control enzymatic activity in a dose-dependent manner, being HT the more effective one; its *in vivo* metabolite HA still retains the biological activity of its dietary precursor. Significant protection is also exerted by TYR despite its weak scavenging activity, indicating that additional mechanisms are involved in the protective effect [42].

As described previously, ATP11C is an ATP-dependent enzyme, while PLSCR1 is Ca^{2+}-dependent enzyme. Consequently, we tried to explore whether alteration in Ca^{2+} and ATP intracellular levels could be partially responsible for the reported changes in the enzymatic activities. In our experimental conditions, intracellular Ca^{2+} levels did not vary, according to our previous report indicating that the selected phenols mainly act on Ca^{2+}-independent mechanisms [13]. Conversely, a significant decrease in intracellular ATP occurs in $HgCl_2$-treated RBC. All the tested phenols were able to fully restore ATP levels at a concentration as low as 5 μM. Therefore, this could represent a key mechanism of the mechanisms underlying both the change in flippase activity following $HgCl_2$-treatment as well as the protective effect observed. It has been demonstrated that Hg^{2+} can significantly influence the activity of several enzymes involved in glycolysis, including hexokinase and phosphofructokinase [43]. Additionally, it has been reported that HT can induce an increase in glycolytic flux in several model systems [44, 45].

The data obtained from Western blotting analysis allow us to indicate a further mechanism. In this respect, we report that $HgCl_2$ treatment induced a decrease in the intensity of the band related to ATP11C, while an increase in intensity was detected for PLSCR1. These data are in line with those obtained for the variation of enzymatic activity. In this case too, treatment with all phenolic compounds showed protective effect. It should be underlined that while phenols pre-treatment results in an almost complete recovery of the intensity of ATP11C band the protective effect exerted on PLSCR1 appears less effective.

It is well known that Hg^{2+} treatment induces the stirring of the cell membrane leading to the contraction of RBC and consequently microvesicle (MV) generation [46]. Interestingly, using spin-labelled or radioisotope-labelled phospholipids, ATP-dependent enzymes were identified in RBC-derived MV [9]. Furthermore, *Seki* et al. [19] showed the presence of ATP11C on artificially produced MV. This could be a mechanism to explain the reduction in the intensity of the ATP11C-associated band under our conditions. In this respect, in a previous work we showed how olive oil phenols were able to determine a notable reduction of $HgCl_2$-induced MV generation [13]. Therefore, it

is conceivable that the protective effect could also be related to the reduction in the number of MV produced.

Regarding the scramblase PLSCR1, it has been reported that this enzyme is found in so-called lipid rafts and that its anchoring to the membrane is regulated by palmitoylation [47–50]. In addition, previous studies have shown that other RBC membrane proteins present in lipid rafts, such as flotillin and ankyrin, are altered after treatment with $HgCl_2$ [21], with an increase in membrane expression levels. The presence of the metal, by interacting with thiol groups, could alter the association of these proteins with the membrane and their mutual interactions, leading to significant changes in the lateral organization of the plasma membrane. In addition, it is noteworthy that $HgCl_2$ has been reported to induce conformational changes in this enzyme, associated with protein self-aggregation [51]. These observations suggest that the presence of $HgCl_2$ could influence various processes, resulting in increased exposure of PLSCR1 on the cell membrane.

Another hypothesis is based on the identification of specific processes in which the activities of flippase and scramblase are closely linked. In this respect, *Nagata* et al. [9] demonstrated that under certain circumstances, a decrease in flippase activity leads to the subsequent activation of scramblase. This might suggest that also under conditions of high stress, such as the one induced by $HgCl_2$-treatment, a similar mechanism could occur in which the enzymatic activity of scramblase is influenced by flippase inhibition. The mechanism behind the protective effect, however, remains to be understood.

Additionally, an interesting finding is that all tested compounds are able to maintain cellular thiols homeostasis, counteracting GSH depletion in $HgCl_2$-exposed RBC. Our team previously demonstrated that olive oil phenols were able to reduce GSH depletion induced by $HgCl_2$-treatment [13]. Remarkably, we have now observed that this protective effect manifests within just 1 h of treatment and at low concentrations. The rapidity of this process prompts us to propose it as one of the molecular mechanisms underpinning the observed protection. The scavenging activity enable polyphenols to neutralize free radicals and reduce oxidative stress thus reducing the demand for GSH, allowing its intracellular levels to be maintained. In addition, these compounds can act as electron donors in redox processes, helping to convert glutathione radical back into its reduced form. This proposed regeneration cycle could allow for maintaining of high GSH levels in cells. Finally, the effect of these compounds on increasing the activity of enzymes involved in restoring reduced GSH levels, such as GSH reductase, could not be ruled out similarly to what is reported for different antioxidants [52].

It is established that while elevated GSH levels can shield RBC from Hg toxicity, prolonged exposure may compromise RBC viability and trigger prothrombotic activity, which could also impact CVD. In fact, there is a great deal of evidence supporting the role of GSH depletion in atherosclerotic progression [53]. Indeed, GSH has been found to be directly linked to the prevention of thrombosis and thrombotic events through numerous mechanisms [54]. In particular, it protects against the damaging effects of free radicals that can damage endothelial cells, contributing to vasodilation and preventing platelets, modulating their aggregation, and leucocytes from adhering to the vascular wall [55,56]. GSH is also involved in modulating inflammation and immune response [57].

Finally, results obtained from molecular modeling provided further insights into the potential mechanism of action of HT on flippase activity. It is well-established that Mg^{2+} ions regulate flippase activity by coordinating the α- and β-phosphates of ADP, thereby compensating for the negative electrostatics of the phosphate groups and catalyzing phosphoryl transfer.

Hg^{2+} is known to disrupt protein function through binding to cysteine residues, often impacting various enzymatic activities. In our study, we analyzed the ATP11C protein sequence to identify cysteine residues with high solvent accessibility that could serve as Hg^{2+} binding sites. Our results highlight C184, a cysteine situated in a solvent-accessible area near the Mg^{2+} pocket, as a notable candidate. The strategic positioning of C184 suggests that Hg^{2+} binding here may interfere with Mg^{2+} interactions, potentially impacting flippase activity.

HT has been shown to possess chelating properties for iron [58], suggesting that the protective effect of HT and other phenols studied may partly involve metal chelation, thereby hindering Hg^{2+} interference. Furthermore, molecular modeling studies suggested direct binding of HT with the Mg^{2+} pocket within the protein, where the C184 is also found. The binding pose observed resembles a protective layer over the pocket, potentially shielding C184 from Hg^{2+} interference. Thus, HT could potentially shield Mg^{2+} functioning in two ways: first, by physically binding within the Mg^{2+} pocket, thus protecting C184 from Hg^{2+} binding, and second, by chelating the metal ion, which might indirectly reduce Hg^{2+}'s ability to disrupt Mg^{2+} function. These findings point to a dual mechanism through which HT could exert a protective effect, though experimental validation is needed to confirm these interactions and their impact on flippase activity.

The movement of lipids across the plasma membrane is an extremely complex process, that regulates the physiological lipidic asymmetry of cell membrane, crucial for many aspects of cell biology, including cell signaling, cell adhesion and response to environmental stresses [59]. In RBC the externalization of PS to the outer leaflet of the cell membrane is a key event associated with the programmed cell death of these cells, also called eryptosis. This process plays a key role in the removal of aged and/or damaged cells, contributing to the overall health of the body [60,61]. Eryptosis also prevents intravascular hemolysis of RBC, allowing them to be eliminated without causing membrane rupture and subsequent inflammation due to the release of intracellular contents [27]. Alteration in this process, however, may contribute to pathological conditions such as endothelial dysfunction and thrombotic events [62]. The possibility that these compounds could prevent alterations in the physiological membrane asymmetry induced by different stressor and/or pathological situations deserve further investigation.

5. Conclusion

Previous studies from our group have sustained the protective property of structurally related olive oil phenols in preventing PS externalization in RBC membrane induced by different stressor, including Hg. In the present study we aimed to elucidate the possible mechanisms underlying the protective effect. Based on the presented data we conclude that preincubation of human RBC with olive oil antioxidant phenols affect phospholipid translocase activities, acting in multifactorial ways, being the protective effect more effective for ATP11C. Performing *in vivo* studies in animal models, such as mice exposed to Hg, would indeed be the next step to confirm and expand upon our *ex vivo* findings.

Altogether, finding presented in this paper and previous reports provide experimental evidence that plant-derived compounds, normally present in our diet, especially the Mediterranean Diet, have the potential to mitigate heavy metal-induced RBC dysfunction, therefore representing ideal candidates for nutritional/nutraceutical strategies to counteract the clinical outcomes of chronic Hg exposure in humans, particularly related to prevention of CVD.

CRediT authorship contribution statement

Pasquale Perrone: Writing – original draft, Visualization, Validation, Investigation, Formal analysis, Conceptualization. **Rosaria Notariale:** Investigation, Formal analysis, Conceptualization. **Gennaro Lettieri:** Visualization, Software. **Luigi Mele:** Investigation, Formal analysis. **Valeria La Pietra:** Writing – original draft, Visualization, Software, Formal analysis. **Marina Piscopo:** Writing – review & editing, Formal analysis. **Caterina Manna:** Writing – review & editing, Writing – original draft, Validation, Supervision, Methodology, Conceptualization.

Funding sources

This research did not receive any specific grant from funding agencies in the public, commercial, or not-for-profit sectors.

Declaration of competing interest

The authors declare that no conflict of interest exists.

Appendix A. Supplementary data

Supplementary data to this article can be found online at https://doi.org/10.1016/j.freeradbiomed.2024.11.047.

References

[1] S.A. Alghareeb, M.A. Alfhili, S. Fatima, Molecular mechanisms and pathophysiological significance of eryptosis, Int. J. Mol. Sci. 24 (2023) 5079, https://doi.org/10.3390/ijms24065079.
[2] P.A. Leventis, S. Grinstein, The distribution and function of phosphatidylserine in cellular membranes, Annu. Rev. Biophys. 39 (2010) 407–427, https://doi.org/10.1146/annurev.biophys.093008.131234.
[3] C.F. Arias, C.F. Arias, How do red blood cells know when to die? R. Soc. Open Sci. 4 (2017) 160850 https://doi.org/10.1098/rsos.160850.
[4] M. Moras, S.D. Lefevre, M.A. Ostuni, From erythroblasts to mature red blood cells: organelle clearance in mammals, Front. Physiol. 8 (2017) 1076, https://doi.org/10.3389/fphys.2017.01076.
[5] N. Arashiki, Y. Takakuwa, Maintenance and regulation of asymmetric phospholipid distribution in human erythrocyte membranes: implications for erythrocyte functions, Curr. Opin. Hematol. 24 (2017) 167–172, https://doi.org/10.1097/MOH.0000000000000326.
[6] J.W. Weisel, R.I. Litvinov, Red blood cells: the forgotten player in hemostasis and thrombosis, J. Thromb. Haemostasis 17 (2019) 271–282, https://doi.org/10.1111/jth.14360.
[7] C. Closse, J. Dachary-Prigent, M.R. Boisseau, Phosphatidylserine-related adhesion of human erythrocytes to vascular endothelium, Br. J. Haematol. 107 (1999) 300–302, https://doi.org/10.1046/j.1365-2141.1999.01718.x.
[8] M.H.A.M. Fens, R. van Wijk, G. Andringa, K.L. van Rooijen, H.M. Dijstelbloem, J. T. Rasmussen, K.M.K. de Vooght, R.M. Schiffelers, C.A.J.M. Gaillard, W.W. van Solinge, A role for activated endothelial cells in red blood cell clearance: implications for vasopathology, Haematologica 97 (2012) 500–508, https://doi.org/10.3324/haematol.2011.048694.
[9] S. Nagata, T. Sakuragi, K. Segawa, Flippase and scramblase for phosphatidylserine exposure, Curr. Opin. Immunol. 62 (2020) 31–38, https://doi.org/10.1016/j.coi.2019.11.009.
[10] K.M. Kodigepalli, K. Bowers, A. Sharp, M. Nanjundan, Roles and regulation of phospholipid scramblases, FEBS Lett. 589 (2015) 3–14, https://doi.org/10.1016/j.febslet.2014.11.036.
[11] J.P. Andersen, A.L. Vestergaard, S.A. Mikkelsen, L.S. Mogensen, M. Chalat, R. S. Molday, P4-ATPases as phospholipid flippases-structure, function, and enigmas, Front. Physiol. 7 (2016) 275, https://doi.org/10.3389/fphys.2016.00275.
[12] N. Arashiki, Y. Takakuwa, N. Mohandas, J. Hale, K. Yoshida, H. Ogura, T. Utsugisawa, S. Ohga, S. Miyano, S. Ogawa, S. Kojima, H. Kanno, ATP11C is a major flippase in human erythrocytes and its defect causes congenital hemolytic anemia, Haematologica 101 (2016) 559–565, https://doi.org/10.3324/haematol.2016.142273.
[13] R. Notariale, P. Perrone, L. Mele, G. Lettieri, M. Piscopo, C. Manna, Olive oil phenols prevent mercury-induced phosphatidylserine exposure and morphological changes in human erythrocytes regardless of their different scavenging activity, Int. J. Mol. Sci. 23 (2022) 5693, https://doi.org/10.3390/ijms23105693.
[14] A. Prüss-Ustün, C. Vickers, P. Haefliger, R. Bertollini, Knowns and unknowns on burden of disease due to chemicals: a systematic review, Environ. Health 10 (2011) 9, https://doi.org/10.1186/1476-069X-10-9.
[15] R. Notariale, R. Infantino, E. Palazzo, C. Manna, Erythrocytes as a model for heavy metal-related vascular dysfunction: the protective effect of dietary components, Int. J. Mol. Sci. 22 (2021) 6604, https://doi.org/10.3390/ijms22126604.
[16] L.E. Hernández, J. Sobrino-Plata, M.B. Montero-Palmero, S. Carrasco-Gil, M. L. Flores-Cáceres, C. Ortega-Villasante, C. Escobar, Contribution of glutathione to the control of cellular redox homeostasis under toxic metal and metalloid stress, J. Exp. Bot. 66 (2015) 2901–2911, https://doi.org/10.1093/jxb/erv063.
[17] K.-M. Lim, S. Kim, J.-Y. Noh, K. Kim, W.-H. Jang, O.-N. Bae, S.-M. Chung, J.-H. Chung, Low-level mercury can enhance procoagulant activity of erythrocytes: a new contributing factor for mercury-related thrombotic disease, Environ. Health Perspect. 118 (2010) 928–935, https://doi.org/10.1289/ehp.0901473.
[18] P. Perrone, S. Spinelli, G. Mantegna, R. Notariale, E. Straface, D. Caruso, G. Falliti, A. Marino, C. Manna, A. Remigante, R. Morabito, Mercury chloride affects band 3 protein-mediated anionic transport in red blood cells: role of oxidative stress and protective effect of olive oil polyphenols, Cells 12 (2023) 424, https://doi.org/10.3390/cells12030424.
[19] M. Seki, N. Arashiki, Y. Takakuwa, K. Nitta, F. Nakamura, Reduction in flippase activity contributes to surface presentation of phosphatidylserine in human senescent erythrocytes, J. Cell Mol. Med. 24 (2020) 13991–14000, https://doi.org/10.1111/jcmm.16010.
[20] A. Officioso, K. Alzoubi, F. Lang, C. Manna, Hydroxytyrosol inhibits phosphatidylserine exposure and suicidal death induced by mercury in human erythrocytes: possible involvement of the glutathione pathway, Food Chem. Toxicol. 89 (2016) 47–53, https://doi.org/10.1016/j.fct.2016.01.003.
[21] R. Notariale, E. Längst, P. Perrone, D. Crettaz, M. Prudent, C. Manna, Effect of mercury on membrane proteins, anionic transport and cell morphology in human erythrocytes, Cell. Physiol. Biochem. 56 (2022) 500–513, https://doi.org/10.33594/000000572.
[22] F. Tortora, R. Notariale, V. Maresca, K.V. Good, S. Sorbo, A. Basile, M. Piscopo, C. Manna, Phenol-rich feijoa sellowiana (pineapple guava) extracts protect human red blood cells from mercury-induced cellular toxicity, Antioxidants 8 (2019) 220, https://doi.org/10.3390/antiox8070220.
[23] E.F. Pettersen, T.D. Goddard, C.C. Huang, G.S. Couch, D.M. Greenblatt, E.C. Meng, T.E. Ferrin, UCSF Chimera–a visualization system for exploratory research and analysis, J. Comput. Chem. 25 (2004) 1605–1612, https://doi.org/10.1002/jcc.20084.
[24] H. Nakanishi, T. Nishizawa, K. Segawa, O. Nureki, Y. Fujiyoshi, S. Nagata, K. Abe, Transport cycle of plasma membrane flippase ATP11C by Cryo-EM, Cell Rep. 32 (2020) 108208, https://doi.org/10.1016/j.celrep.2020.108208.
[25] R.A. Friesner, R.B. Murphy, M.P. Repasky, L.L. Frye, J.R. Greenwood, T.A. Halgren, P.C. Sanschagrin, D.T. Mainz, Extra precision glide: docking and scoring incorporating a model of hydrophobic enclosure for protein-ligand complexes, J. Med. Chem. 49 (2006) 6177–6196, https://doi.org/10.1021/jm051256o.
[26] Glide: a new approach for rapid, accurate docking and scoring. 2. Enrichment factors in database screening - PubMed, (n.d.). https://pubmed.ncbi.nlm.nih.gov/15027866/(accessed March 27, 2024).
[27] I. Restivo, A. Attanzio, L. Tesoriere, M. Allegra, G. Garcia-Llatas, A. Cilla, Anti-eryptotic activity of food-derived phytochemicals and natural compounds, Int. J. Mol. Sci. 23 (2022) 3019, https://doi.org/10.3390/ijms23063019.
[28] L. Martínez-Zamora, R. Peñalver, G. Ros, G. Nieto, Olive tree derivatives and hydroxytyrosol: their potential effects on human health and its use as functional ingredient in meat, Foods 10 (2021) 2611, https://doi.org/10.3390/foods10112611.
[29] N.D. Utami, A. Nordin, H. Katas, R. Bt Hj Idrus, M.B. Fauzi, Molecular action of hydroxytyrosol in wound healing: an in vitro evidence-based review, Biomolecules 10 (2020) 1397, https://doi.org/10.3390/biom10101397.
[30] G. Serreli, M. Deiana, Extra virgin olive oil polyphenols: modulation of cellular pathways related to oxidant species and inflammation in aging, Cells 9 (2020) 478, https://doi.org/10.3390/cells9020478.
[31] R. Moral, E. Escrich, Influence of olive oil and its components on breast cancer: molecular mechanisms, Molecules 27 (2022) 477, https://doi.org/10.3390/molecules27020477.
[32] A. Sain, S. Sahu, D. Naskar, Potential of olive oil and its phenolic compounds as therapeutic intervention against colorectal cancer: a comprehensive review, Br. J. Nutr. 128 (2022) 1257–1273, https://doi.org/10.1017/S0007114521002919.
[33] M. Farràs, E. Almanza-Aguilera, Á. Hernáez, N. Agustí, J. Julve, M. Fitó, O. Castañer, Beneficial effects of olive oil and Mediterranean diet on cancer physiopathology and incidence, Semin. Cancer Biol. 73 (2021) 178–195, https://doi.org/10.1016/j.semcancer.2020.11.011.
[34] J. Torić, A.K. Marković, C.J. Brala, M. Barbarić, Anticancer effects of olive oil polyphenols and their combinations with anticancer drugs, Acta Pharm. 69 (2019) 461–482, https://doi.org/10.2478/acph-2019-0052.
[35] L. Micheli, L. Bertini, A. Bonato, N. Villanova, C. Caruso, M. Caruso, R. Bernini, F. Tirone, Role of hydroxytyrosol and oleuropein in the prevention of aging and related disorders: focus on neurodegeneration, skeletal muscle dysfunction and gut microbiota, Nutrients 15 (2023) 1767, https://doi.org/10.3390/nu15071767.
[36] R. Hornedo-Ortega, A.M. Espinosa-Oliva, Hydroxytyrosol and Parkinson's disease: protective actions against alpha-synuclein toxicity, Neural Regen Res 19 (2024) 1427–1428, https://doi.org/10.4103/1673-5374.387987.
[37] C. Noguera-Navarro, S. Montoro-García, E. Orenes-Piñero, Hydroxytyrosol: its role in the prevention of cardiovascular diseases, Heliyon 9 (2023) e12963, https://doi.org/10.1016/j.heliyon.2023.e12963.
[38] M.A. Carluccio, R. Martinelli, M. Massaro, N. Calabriso, E. Scoditti, M. Maffia, T. Verri, V. Gatta, R. De Caterina, Nutrigenomic effect of hydroxytyrosol in vascular endothelial cells: a transcriptomic profile analysis, Nutrients 13 (2021) 3990, https://doi.org/10.3390/nu13113990.
[39] M. Domenech, R. Casas, A.M. Ruiz-León, J. Sobrino, E. Ros, R. Estruch, Effects of a novel nutraceutical combination (Aquilea Colesterol®) on the lipid profile and inflammatory biomarkers: a randomized control trial, Nutrients 11 (2019) 949, https://doi.org/10.3390/nu11050949.
[40] J.-H. Shin, K.-M. Lim, J.-Y. Noh, O.-N. Bae, S.-M. Chung, M.-Y. Lee, J.-H. Chung, Lead-induced procoagulant activation of erythrocytes through phosphatidylserine exposure may lead to thrombotic diseases, Chem. Res. Toxicol. 20 (2007) 38–43, https://doi.org/10.1021/tx060114+.
[41] B. Jn, B. Mj, Exposure to air pollution increases the incidence of hypertension and diabetes in black women living in Los Angeles, J. Clin. Hypertens. 14 (2012), https://doi.org/10.1111/jch.12000.
[42] C. Manna, S. D'Angelo, V. Migliardi, E. Loffredi, O. Mazzoni, P. Morrica, P. Galletti, V. Zappia, Protective effect of the phenolic fraction from virgin olive oils against oxidative stress in human cells, J. Agric. Food Chem. 50 (2002) 6521–6526, https://doi.org/10.1021/jf020565+.
[43] M.J. Ramírez-Bajo, P. de Atauri, F. Ortega, H.V. Westerhoff, J.L. Gelpí, J. J. Centelles, M. Cascante, Effects of cadmium and mercury on the upper part of

skeletal muscle glycolysis in mice, PLoS One 9 (2014) e80018, https://doi.org/10.1371/journal.pone.0080018.
[44] M. Garcia-Guasch, E. Escrich, R. Moral, I.F. Duarte, Metabolomics Insights into the differential response of breast cancer cells to the phenolic compounds hydroxytyrosol and luteolin, Molecules 28 (2023) 3886, https://doi.org/10.3390/molecules28093886.
[45] X. Zhan, M. He, J. Pei, W. Fan, C.N. Mwangi, P. Zhang, X. Chai, M. Jiang, Natural phenylethanoid supplementation alleviates metabolic syndrome in female mice induced by high-fructose diet, Front. Pharmacol. 13 (2022) 850777, https://doi.org/10.3389/fphar.2022.850777.
[46] R. Bissinger, A.A.M. Bhuyan, S.M. Qadri, F. Lang, Oxidative stress, eryptosis and anemia: a pivotal mechanistic nexus in systemic diseases, FEBS J. 286 (2019) 826–854, https://doi.org/10.1111/febs.14606.
[47] T. Wiedmer, J. Zhao, M. Nanjundan, P.J. Sims, Palmitoylation of phospholipid scramblase 1 controls its distribution between nucleus and plasma membrane, Biochemistry 42 (2003) 1227–1233, https://doi.org/10.1021/bi026679w.
[48] J. Zhao, Q. Zhou, T. Wiedmer, P.J. Sims, Palmitoylation of phospholipid scramblase is required for normal function in promoting Ca2+-activated transbilayer movement of membrane phospholipids, Biochemistry 37 (1998) 6361–6366, https://doi.org/10.1021/bi980218m.
[49] S. Rayala, U. Sivagnanam, S.N. Gummadi, Biophysical characterization of the DNA binding motif of human phospholipid scramblase 1, Eur. Biophys. J. 51 (2022) 579–593, https://doi.org/10.1007/s00249-022-01621-0.
[50] J. Sun, M. Nanjundan, L.J. Pike, T. Wiedmer, P.J. Sims, Plasma membrane phospholipid scramblase 1 is enriched in lipid rafts and interacts with the epidermal growth factor receptor, Biochemistry 41 (2002) 6338–6345, https://doi.org/10.1021/bi025610l.
[51] A.K. Shettihalli, S.N. Gummadi, Biochemical evidence for lead and mercury induced transbilayer movement of phospholipids mediated by human phospholipid scramblase 1, Chem. Res. Toxicol. 26 (2013) 918–925, https://doi.org/10.1021/tx400090h.
[52] R.K. Kempaiah, K. Srinivasan, Antioxidant status of red blood cells and liver in hypercholesterolemic rats fed hypolipidemic spices, Int. J. Vitam. Nutr. Res. 74 (2004) 199–208, https://doi.org/10.1024/0300-9831.74.3.199.
[53] F. Violi, L. Loffredo, R. Carnevale, P. Pignatelli, D. Pastori, Atherothrombosis and oxidative stress: mechanisms and management in elderly, Antioxidants Redox Signal. 27 (2017) 1083–1124, https://doi.org/10.1089/ars.2016.6963.
[54] J. Loscalzo, Oxidative stress in endothelial cell dysfunction and thrombosis, Pathophysiol. Haemostasis Thrombosis 32 (2002) 359–360, https://doi.org/10.1159/000073600.
[55] D.E. Handy, J. Loscalzo, The role of glutathione peroxidase-1 in health and disease, Free Radic. Biol. Med. 188 (2022) 146–161, https://doi.org/10.1016/j.freeradbiomed.2022.06.004.
[56] H. Li, S. Horke, U. Förstermann, Oxidative stress in vascular disease and its pharmacological prevention, Trends Pharmacol. Sci. 34 (2013) 313–319, https://doi.org/10.1016/j.tips.2013.03.007.
[57] I. Glassman, N. Le, M. Mirhosseini, C.A. Alcantara, A. Asif, A. Goulding, S. Muneer, M. Singh, J. Robison, F. Guilford, V. Venketaraman, The role of glutathione in prevention of COVID-19 immunothrombosis: a review, FBL 28 (2023) 59, https://doi.org/10.31083/j.fbl2803059.
[58] T. Hofer, T.Ø. Jørgensen, R.L. Olsen, Comparison of food antioxidants and iron chelators in two cellular free radical assays: strong protection by luteolin, J. Agric. Food Chem. 62 (2014) 8402–8410, https://doi.org/10.1021/jf5022779.
[59] E. Sezgin, I. Levental, S. Mayor, C. Eggeling, The mystery of membrane organization: composition, regulation and roles of lipid rafts, Nat. Rev. Mol. Cell Biol. 18 (2017) 361–374, https://doi.org/10.1038/nrm.2017.16.
[60] A. Tkachenko, Apoptosis and eryptosis: similarities and differences, Apoptosis 29 (2024) 482–502, https://doi.org/10.1007/s10495-023-01915-4.
[61] R. L, J. Am, Eryptosis: an erythrocyte's suicidal type of cell death, BioMed Res. Int. 2018 (2018), https://doi.org/10.1155/2018/9405617.
[62] S.M. Qadri, R. Bissinger, Z. Solh, P.-A. Oldenborg, Eryptosis in health and disease: a paradigm shift towards understanding the (patho)physiological implications of programmed cell death of erythrocytes, Blood Rev. 31 (2017) 349–361, https://doi.org/10.1016/j.blre.2017.06.001.